Available online at www.sciencedirect.com
ScienceDirect
Ceramics International 38S (2012) S485–S488
CERAMICS INTERNATIONAL
www.elsevier.com/locate/ceramint

Fabrication of scandia-stabilized zirconia electrolyte with a porous and dense composite layer for solid oxide fuel cells

Young-Hoon Choi [a,b], Se-Hee Lee [a,c], Jürgen Wackerl [d], Doo-Hwan Jung [a], Dong-Soo Suhr [b], Se-Young Choi [c], Dong-Hyun Peck [a,*]

[a] Korea Institute of Energy Research (KIER), Daejeon 305-343, Republic of Korea
[b] Chungnam National University, Daejeon 305-764, Republic of Korea
[c] Yonsei University, Seoul 120-749, Republic of Korea
[d] Institute of Energy Research, Research Centre Jülich (FZJ), Jülich 52425, Germany

Available online 25 May 2011

Abstract

Scandia-stabilized zirconia (ScSZ) is a new candidate electrolyte for use in solid oxide fuel cells (SOFCs) at intermediate temperatures. ScMnSZ ($(ZrO_2)_{0.89}(Sc_2O_3)_{0.1}(MnO_2)_{0.01}$) powders for the electrolyte were synthesized using the Pechini and ultrasonic spray pyrolysis (USP) methods. The electrical conductivities of sintered ScMnSZ samples prepared by the Pechini and USP methods are determined to be 0.112 and 0.091 S/cm, respectively, at 800 °C. An additional porous ScMnSZ electrolyte layer onto the dense electrolyte layer through a dip-coating process is a possible means of increasing the triple-phase boundary (TPB) of a cell. The performance of an anode-supported single cell prepared using a porous and dense composite electrolyte is superior to that of a cell with only the dense electrolyte.

Keywords: E. fuel cells; Scandia-stabilized zirconia; Solid oxide; Composite electrolyte

1. Introduction

Scandia-stabilized zirconia (ScSZ, $(ZrO_2)_{1-x}(Sc_2O_3)_x$) shows high ionic and low electronic conductivity and high chemical stability. It is a candidate electrolyte for solid oxide fuel cells (SOFCs) at intermediate temperatures [1,2].

The triple-phase boundary (TPB) concept holds that the hydrogen oxidation reaction (HOR) and the oxygen reduction reaction (ORR) can only occur at confined spatial sites, where an electrolyte, an electrode, and a gas come into contact. The performance of SOFC is often limited by the reaction kinetics, especially in ORR. Therefore, optimizing the TPB in the cell is very important to improve the performance of fuel cells [3–5]. The microstructure of the interface between the electrolyte and cathode should be carefully designed to maximize TPB in the electrode. Weber and co-workers [6,7] proposed a method for preparation of an electrochemical active thin film cathode via MOD (metal-organic-deposition) to increase the number of active reaction sites for a SOFC.

In this paper, a preparation method of the electrolyte was developed to increase the active reaction sites in the TPB of a SOFC. ScMnSZ ($(ZrO_2)_{0.89}(Sc_2O_3)_{0.1}(MnO_2)_{0.01}$) powder for a dense and porous additional composite electrolyte layer was synthesized by the Pechini and ultrasonic spray pyrolysis (USP) methods, respectively. The porous electrolyte was coated onto a dense electrolyte layer to increase the effective TPB region and also to improve the performance of the cell. The effective surface area of electrolyte can be increased by its well-developed porous microstructure. The performance of single cells prepared using dense and porous electrolyte composites (cell 2) was compared with the performance of a cell in which only dense electrolyte was used (cell 1).

2. Experimental

The ScMnSZ powder for the dense and porous electrolyte layer was prepared by the Pechini and USP methods, respectively. The ScMnSZ electrolyte material was doped

* Corresponding author. Tel.: +82 42 8603501; fax: +82 42 8603739.
E-mail address: dhpeck@kier.re.kr (D.-H. Peck).

0272-8842/$36.00
doi:10.1016/j.ceramint.2011.05.059

with a small amount (1 mol%) of manganese oxide (MnO_2) for suppression of the cubic-rhombohedral phase transformation [2,8]. The metal nitrates of $Zr(NO_3)_2{\cdot}xHNO_3$ (GCM, Korea), $Sc(NO_3)_2{\cdot}xH_2O$ (GCM, Korea), and $Mn(NO_3)_2{\cdot}4H_2O$ (Sigma–Aldrich Co.) were used for the ScMnSZ electrolyte powders. A 0.5:0.5 molar mixture of citric acid (CA) and ethylene glycol (EG) was added to the nitrate solution. The viscous gel was then charred at 240 °C for 3 h and calcined at 750 °C for 10 h for the Pechini method [2]. The nitrate solution (0.1–0.5 mol/L) was atomized by an ultrasonic nebulizer with a resonant frequency of 1.7 MHz for the USP method. The atomized droplets passed through a quartz tube (50 mm in diameter) heated to 750 °C with a carrier gas (air) and the ScMnSZ powder was collected in a filter bag attached onto end of the quartz tube [2].

The morphology of the powder and the microstructure and chemical composition of the sintered body were investigated using a scanning electron microscope (FE-SEM, HITACHI S–4700) equipped with an energy dispersive X-ray analyzer (EDS). The electrical conductivity of the sintered ScMnSZ samples prepared by the Pechini and USP methods was measured by the DC four-probe method. Thermal expansion of the sintered ScMnSZ samples was measured using a dilatometer (DIL 402C, Netzsch, Germany) in the air atmosphere with a heating rate of 5 °C/min in the temperature range from 300 to 1027 °C.

The extruded anode-supported tube serves as the fuel electrode (Ni/YSZ). The ScMnSZ electrolyte layer using the powder prepared by the Pechini method was coated onto a pre-sintered anode tube by a slurry dip-coating process to form a dense layer. An additional porous electrolyte layer was then coated onto the dense electrolyte by the dip-coating process using a mixture of polymer hollow particles (d_{50} = 0.5 μm) and ScMnSZ powder prepared by the USP method. The coated electrolyte layer was sintered at 1400 °C for 10 h. An air electrode LSM ($(La_{0.85}Sr_{0.15})_{0.9}MnO_3$) was prepared by solid-state powder reaction process and calcined at 1000 °C for 5 h. The air electrode LSM slurry was coated via a dip-coating process onto electrolyte layer and sintered at 1200 °C for 2 h in air.

The electrode area of the single cell was 9.42 cm^2. The cell performance was measured at 800 °C while supplying humidified H_2 (0.7 L/min) with 3 wt% H_2O as fuel and air (3.5 L/min) as an oxidant. AC impedance spectroscopy (Solatron SI 1260/SI 1287) was used to measure the polarization resistance of the single cell in the frequency range from 1×10^5 to 0.01 Hz at signal amplitude of 50 mV AC in the state of open-circuit voltage (OCV).

3. Results and discussion

SEM micrographs of ScMnSZ powder synthesized by the Pechini (a) and USP methods (b) are shown in Fig. 1. The mean particle diameters (d_{50}) of those powders were about 0.35 and 0.67 μm, respectively. The sintered samples prepared by the Pechini method exhibited a relatively dense microstructure, while the microstructure was porous for the sintered sample prepared by the USP method [8].

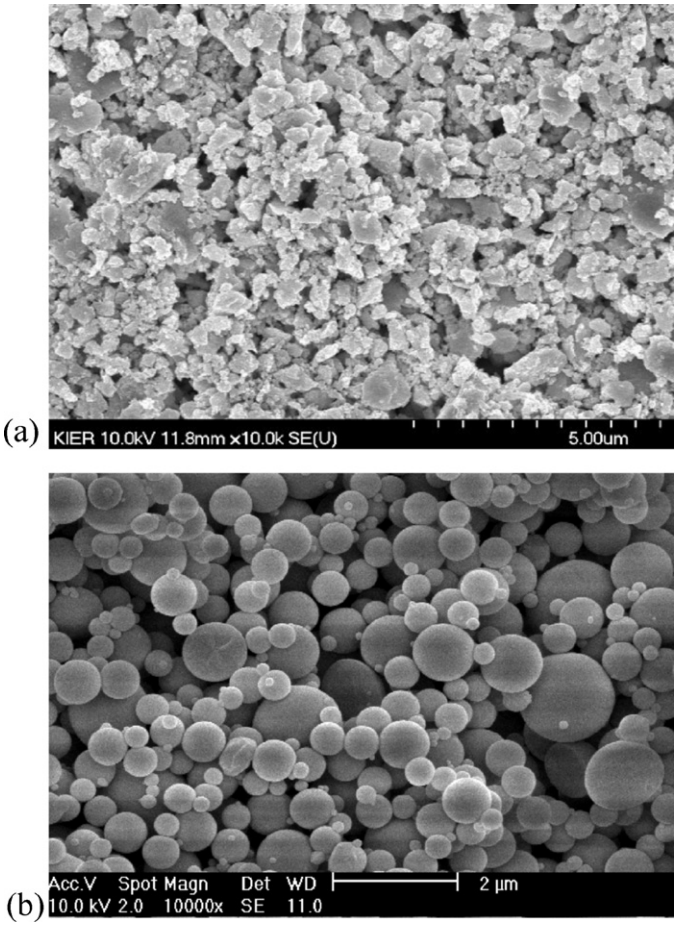

Fig. 1. SEM images of ScMnSZ powder prepared by the Pechini (a) and USP methods (b).

The electrical conductivities of the sintered ScMnSZ samples prepared by the USP methods were 0.054, 0.091 and 0.207 S/cm at 750, 800 and 900 °C, respectively. On the other hand, the sintered sample prepared by the Pechini methods showed the electrical conductivities of 0.074, 0.112 and 0.208 S/cm at 750, 800 and 900 °C, respectively. The electrical conductivity of a sintered sample prepared by the Pechini method was higher than that by the USP method. The conductivity of such samples can be affected by the porosity of the sintered materials [8]. The sintered ScMnSZ samples prepared by the Pechini and USP methods showed a single cubic phase and no detection of a new phase by X-ray diffraction (XRD) analysis. The sintered ScMnSZ sample showed a linear thermal expansion behavior ($\alpha_{tech}(1273\ K) = 10.78 \times 10^{-6}\ (K^{-1})$) in a dilatometer analysis. These results shows that the addition of a small amount (1 mol%) of metal oxides (MnO_2) into the ScSZ material be an effective method for suppression of the cubic-rhombohedral phase transformation of ScSZ materials [2,9].

SEM image of a cross-section of a single cell (cell 2) composed of a dense and porous electrolyte layer (dense electrolyte (A), porous electrolyte (B), and cathode (C)) is shown in Fig. 2(a). The thickness of the dense and additional porous electrolyte layer was about 10–12 and 3–5 μm,

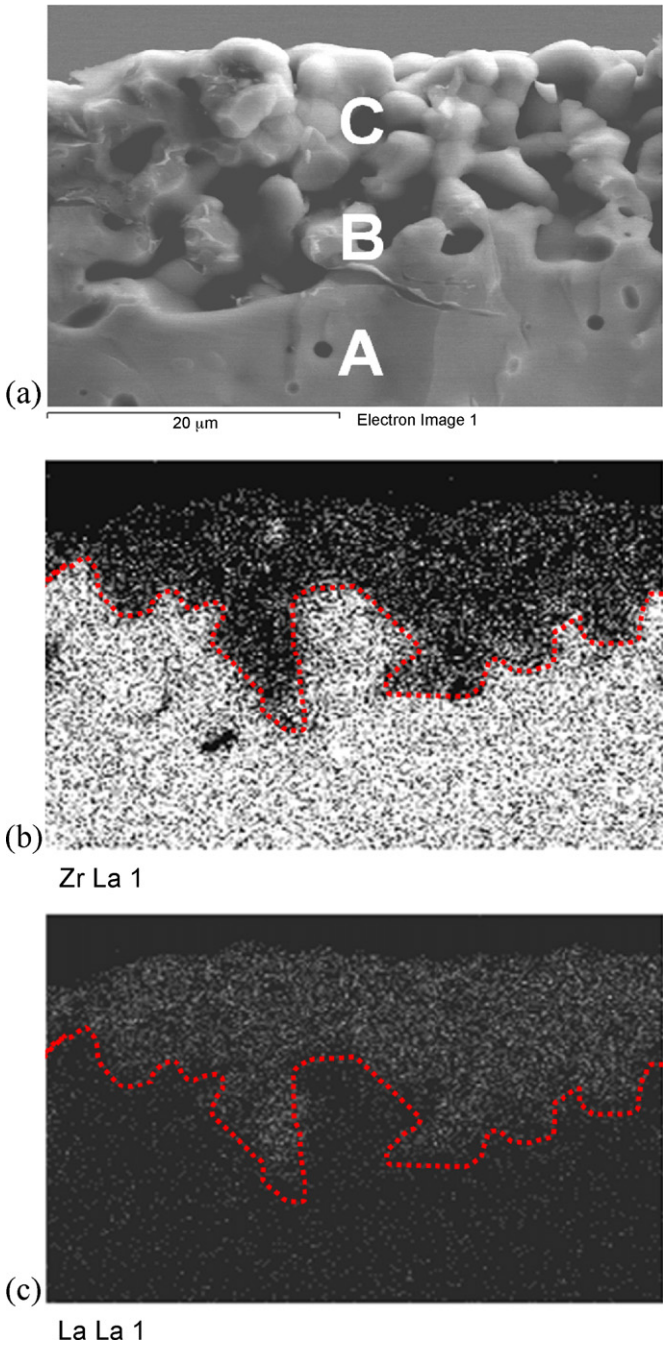

Fig. 2. SEM (a) and X-ray mapping (Zr and La) (b, c) images of a cross-section of a single cell (cell 2) composed of a dense and porous electrolyte layer (dense electrolyte (A), a porous electrolyte (B), and a cathode (C)).

respectively. The cathode shows a porous structure and a thickness of approximately 10–15 μm. The dense and porous electrolyte, and cathode layers are distinguished clearly in the mapping image of the Zr and La elements (Fig. 2 (b) and (c)). The electrolyte surface area and the active reaction sites in the TPB (LSM/ScMnSZ/air) were enlarged by the application of the additional porous electrolyte layer significantly.

Fig. 3 shows the current/voltage (*I*/*V*) and current/power (*I*/*P*) curves of the single cells (cell 1 and 2) at 800 °C. The OCV was 1.13 V for both cells. Cell 1 was also fabricated with a

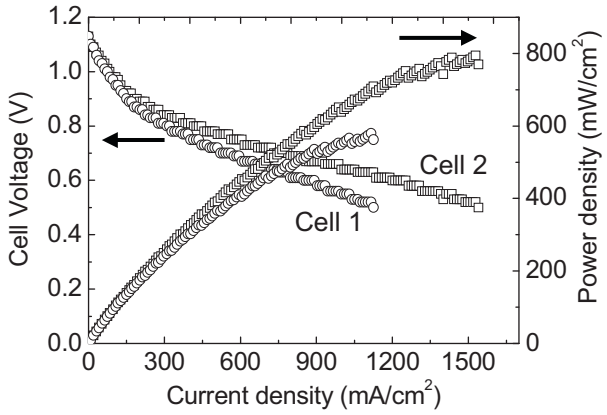

Fig. 3. Current/voltage (*I*/*V*) and current/power (*I*/*P*) curves of a single cell with different electrolyte layers at 800 °C (cell 1, a dense electrolyte layer; cell 2, a dense and porous electrolyte layer).

dense electrolyte layer, but an additional porous electrolyte layer was not applied in the configuration of cell 1. Cell 2 shows a nominal power density of 0.62 W/cm^2 at 0.7 V and a maximum power density of 0.82 W/cm^2 at 0.55 V. Cell 1 shows a nominal power density of 0.39 W/cm^2 at 0.7 V and a maximum power density of 0.58 W/cm^2 at 0.52 V under the same operating conditions as cell 2. Cell 2 shows better performance than cell 1. This improvement can be attributed to the increased length of the TPB in the porous electrolyte and cathode layer [6,7]. An increase in the performance is possible by using an improved electrolyte/cathode interface. The effective electrolyte surface area was enlarged here by structuring the electrolyte surface with additional porous ScMnSZ layers.

The impedance spectra of cells 1 and 2 under air at 800 °C are shown in Fig. 4. The ohmic resistance of cells 1 and 2 was about 0.054 Ω cm^2. A higher polarization resistance of 0.326 Ω cm^2 was obtained for cell 1 with only a dense electrolyte layer; it was 0.264 Ω cm^2 for cell 2 with its dense and porous electrolyte layers. The change in the polarization resistance between cell 1 and cell 2 is clearly visible in Fig. 4. The better performance of cell 2 can be explained by the reduction in the polarization

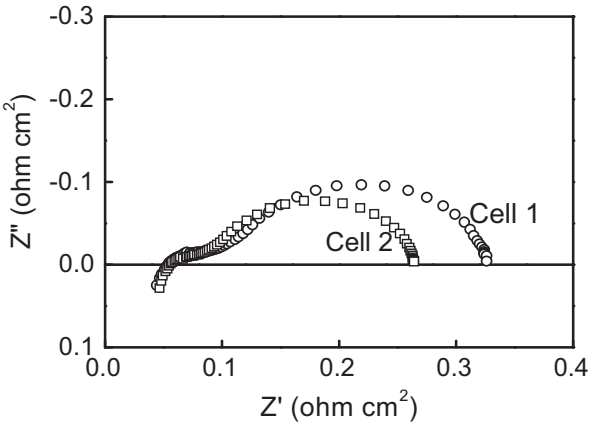

Fig. 4. Impedance spectra in an open-circuit state of a single cell with different electrolyte layers at 800 °C (cell 1, a dense electrolyte layer; cell 2, a dense and porous electrolyte layer).

resistance due to the improved electrical contact between the cathode/electrolyte interlayer [6,7]. The cell performances at 800 °C appear to rely on the electrode polarization resistance more seriously than the ohmic resistance [10].

4. Conclusions

The mean particle diameters of the ScMnSZ powder prepared by the Pechini and USP methods at 750 °C were approximately 0.35 and 0.67 μm, respectively. The electrical conductivities of the sintered ScMnSZ samples prepared by the Pechini and USP methods were 0.112 and 0.091 S/cm at 800 °C, respectively. The nominal power densities of cell 1 and cell 2 were 0.39 and 0.62 W/cm^2 (0.7 V), respectively, at a cell temperature of 800 °C. Cell 2 showed better cell performance than cell 1. This improvement can be attributed to the increased length of the TPB and the lower electrode polarization resistance in the porous electrolyte and cathode layer. Lower electrode polarization resistance of 0.264 Ω cm^2 was obtained for cell 2 with its dense and porous electrolyte layer, while the polarization resistance was 0.326 Ω cm^2 for cell 1 with its dense electrolyte layer.

Acknowledgments

This work was supported by the Joint Research Project under the Korea Research Council for Industrial Science & Technology (ISTK) and for Fundamental Science & Technology (KRCF), Republic of Korea.

References

[1] Y. Arachi, O. Yamamoto, Y. Takeda, N. Imanishi, The electrical conductivity of the ZrO_2–Sc_2O_3–Y_2O_3 and ZrO_2–Sc_2O_3–Yb_2O_3 systems, Denki Gagaku 64 (6) (1996) 638–641.

[2] D.H. Peck, R.H. Song, J.H. Kim, T.H. Lim, D.R. Shin, D.H. Jung, K. Hilpert, Electrical conductivity of scandia stabilized zirconia for membrane in solid oxide fuel cells, in: S.C. Singhal, J. Mizusaki (Eds.),Proceeding of 9th International symposium on solid oxide fuel cells, Pennington, NJ, Electrochemical society (2005) 947–953.

[3] J. Mizusaki, H. Tagawa, K. Tsuneyoshi, A. Sawata, Reaction kinetics and microstructure of the solid oxide fuel cells air electrode $La_{0.6}Ca_{0.4}MnO_3$/YSZ, Journal of the Electrochemical Society 138 (1991) 1867.

[4] A. Bieberle, L.P. Meier, L.J. Gauckler, The electrochemistry of Ni pattern anodes used as solid oxide fuel cell model electrodes, Journal of the Electrochemical Society 148 (2001) A646.

[5] J. Fleig, On the width of the electrochemically active region in mixed conducting solid oxide fuel cell cathodes, Journal of Power Sources 105 (2002) 228.

[6] E. Ivers-Tiffée, A. Weber, D. Herbstritt, Materials and technologies for SOFC-components, Journal of the European Ceramic Society 21 (2001) 1805–1811.

[7] A. Weber, E. Ivers-Tiffée, Materials and concepts for solid oxide fuel cells in stationary and mobile applications, Journal of Power Sources 127 (2004) 273–283.

[8] O.H. Kwon, G.M. Choi, Electrical conductivity of thick film YSZ, Solid State Ionics 177 (2006) 3057.

[9] J.V. Herle, R. Vasquez, Conductivity of Mn and Ni-doped stabilized zirconia electrolyte, Journal of the European Ceramic Society 24 (2004) 1177–1180.

[10] Z. Wang, M. Cheng, Y. Dong, M. Zhang, H. Zhang, Investigation of $LSM_{1.1}$–ScSZ composite cathodes for anode-supported solid oxide fuel cells, Solid State Ionics 176 (2005) 1561–2555.